

Macromolecules

Volume 29, Number 14

July 1, 1996

© Copyright 1996 by the American Chemical Society

Biodegradation of Novel Optically Active Polyesters Synthesized by Copolymerization of (*R*)-MOHEL with Lactones

Hiroyuki Shirahama, Masaki Shiomi, Masanori Sakane, and Hajime Yasuda*

Department of Applied Chemistry, Faculty of Engineering, Hiroshima University, Higashi-Hiroshima 739, Japan

Received November 28, 1995; Revised Manuscript Received April 22, 1996[®]

ABSTRACT: Biodegradations of random copolymers of (*R*)-3-methyl-4-oxa-6-hexanolide [(*R*)-MOHEL] with various lactones such as ϵ -caprolactone (24/76 ratio), δ -valerolactone (22/78), and β -propiolactone (31/69) were examined with normal or acclimated activated sludge. As a consequence, the biodegradability was found to increase in the order poly[(*R*)-MOHEL-*ran*- ϵ -caprolactone] > poly[(*R*)-MOHEL-*ran*- δ -valerolactone] > poly[(*R*)-MOHEL-*ran*- β -propiolactone]. The mode of biodegradation of (*R*)-MOHEL/lactone copolymers with enzymes (cholesterol esterase etc.) resembles that of biodegradation with activated sludge. All the copolymers degraded better than the homopoly[(*R*)-MOHEL] or homopoly(lactone)s. In contrast, these latter polymers are inert to hydrolytic degradation by basic or acidic buffer solution. The major biodegradation product of poly[(*R*)-MOHEL-*ran*- ϵ -caprolactone] (15/85) by enzymes is 6-hydroxycaproic acid as revealed by NMR spectroscopy and mass spectrometry, while the biodegradation product from poly[(*R*)-MOHEL-*ran*- δ -valerolactone] (18/82) is a linear δ -valeric acid dimer.

Introduction

Condensation polymerizations of 3-hydroxyalkanoates as well as ring-opening polymerizations of lactones such as ϵ -caprolactone (CL), δ -valerolactone (VL), and β -propiolactone (PL) provide a convenient route to biodegradable polyesters which are of great interest for a variety of practical applications, e.g., applications in packaging and discardable container industries¹ and medical field applications such as controlled release drug formulations,² surgical sutures,³ and joining materials for bones.⁴ Syntheses of high molecular weight polymers of these lactones have been achieved by using initiators including alkali metals,⁵ alkaline earth metals,⁵ $\text{AlR}_3\text{-H}_2\text{O}$,⁶ (porphyrinato)aluminum,⁷ dialkylzinc- H_2O ,⁸ and CpTi(OR)Cl_2 ⁹ systems. Among these initiators, only the (porphyrinato)aluminum compounds provide polyesters with very narrow molecular weight distributions. Recently organolanthanide(III)¹⁰ and organolanthanide(II) complexes¹¹ were found to exhibit good catalysis for living polymerization of these monomers. Enzymatic synthesis of poly(ϵ -caprolactone) gives low molecular weight polymers with rather low polydispersity.¹² More recently, high molecular weight polymers of (*R*)- β -butyrolactone and high molecular weight copolymers of (*R*)- β -butyrolactone/(*R*)-MOHEL were synthesized using

a ditanoxane as an initiator.¹³ This paper deals with the synthesis of homopoly[(*R*)-3-methyl-4-oxa-6-hexanolide] [(*R*)-MOHEL], random and block copolymers of (*R*)-MOHEL with various lactones, and their special behaviors of biodegradation by normal or acclimated activated sludges as well as by several enzymes.

Results and Discussion

Synthesis of Copolyesters of (*R*)-MOHEL with Lactones. The homopolymerization of a new type of seven-membered lactone, (*R*)-3-methyl-4-oxa-6-hexanolide [(*R*)-MOHEL], was conducted with $\text{AlEt}_3\text{-H}_2\text{O}$ (1/0.8 molar ratio) initiator in toluene at 60 °C for 10 days, and the resulting polymer ($M_n = 190\,000\text{--}230\,000$, $M_w/M_n = \text{ca. } 1.64$) was poured into MeOH (100 mL) to induce the precipitation of polymers. The poly[(*R*)-MOHEL] exhibits a T_g (glass transition point) of -41 °C but does not show a clear T_m (melting point); hence these polymers lack film formation ability at ambient temperature irrespective of their high molecular weights. Since we were seeking elastic polymer films, we carried out copolymerizations of (*R*)-MOHEL with various lactones such as CL, VL, and PL using $\text{AlEt}_3\text{-H}_2\text{O}$ (1/0.8) initiator. Random copolymerization of (*R*)-MOHEL with CL by 50/50, 25/75, 5/95, and 0/100 mol/mol feed ratios gave polymers ($M_n = 110\text{--}291 \times 10^3$, $M_w/M_n = 1.64\text{--}1.75$) of 48/52, 24/76, 4/96, and 0/100 constitution, and these polymers exhibit T_g s of -60.5 , -61.5 , -61.5 ,

[®] Abstract published in *Advance ACS Abstracts*, June 1, 1996.

Table 1. Thermal Properties of MOHEL/Lactone Random Copolymers

polymer (molar ratio)	$M_n/10^{-3}$	T_g (°C)	T_m (°C)	T_d (°C)	crystallinity/%
poly[(<i>R</i>)-MOHEL]	118	-40.6		208	
poly[(<i>S</i>)-MOHEL]	231	-41.1		207	
poly[(<i>RS</i>)-MOHEL]	327	-40.5		209	
poly[(<i>R</i>)-MOHEL/CL]					
(48/52)	283	-60.5	28.9	264	5
(24/76)	291	-61.5	37.5	270	19
(14/86)	248	-61.2	51.3	270	33
(4/96)	279	-61.5	62.0	270	46
poly(CL)	110	-67.0	63.2	275	67
poly[(<i>R</i>)-MOHEL/VL]					
(62/38)	138	-50.0		226	
(35/65)	126	-52.2	38.4	217	
(22/78)	350	-57.5	43.8	210	
poly(VL)	71	-80.1	60.0	210	
poly[(<i>R</i>)-MOHEL/PL]					
(60/40)	107	-36.0	74.5	255	17
(19/81)	82	-21.2	74.0	249	52
poly(PL)	69	-11.8	78.0	249	62

and -67.0 °C, respectively, and T_m s of 28.9, 37.5, 62.0, and 63.2 °C as revealed by DSC measurements (Table 1). Their crystallinities are 5%, 19%, 46%, and 67%, respectively, based on the heat of fusion. T_d s (decomposition points) are 264, 270, 270, and 275 °C. The random copolymers of (*R*)-MOHEL with VL ($M_n = 71-350 \times 10^3$, $M_w/M_n = 1.65-1.70$) synthesized by 25/75, 18/82, and 0/100 mol/mol feed ratios (polymer constitution of 35/65, 22/78, and 0/100) exhibit T_g s of -52.2, -57.5, and -80.1 °C and T_m s of 38.4, 43.8, and 60.0 °C, respectively. Their crystallinities were not clear, and T_d s are 217, 210, and 210 °C, respectively. The random copolymerization of (*R*)-MOHEL with PL by 78/22, 53/47, 27/73, and 0/100 mol/mol feed ratios gave polymers of 81/19, 60/40, 19/81, and 0/100 constitution ($M_n = 69-107 \times 10^3$, $M_w/M_n = 1.45-1.82$), and these polymers exhibit T_g s of -39.4, -36.0, -21.2, and -11.8 °C and T_m s of 67.2, 74.5, 74.0, and 78.0 °C, respectively.

Tensile strengths and elongations of (*R*)-MOHEL-*ran*-CL (11/89), (*R*)-MOHEL-*ran*-VL (9/91), and (*R*)-MOHEL-*ran*-PL (19/81) random copolymers are 30 900, 31 200, and 25 800 kgf/cm² and 1280%, 1010%, and 860%, respectively. These values are higher than the values of low density polyethylene (11000-12000 kgf/cm²), but these are lower than that of polyethylene terephthalate (100000 kgf/cm²).

By using the Fineman-Ross equation, respective monomer reactivity ratios were estimated based on the copolymer composition curve. For the copolymerization of (*R*)-MOHEL with CL, $r_1 = 0.81$ and $r_2 = 0.99$ values were obtained. For the copolymerization of (*R*)-MOHEL with VL, $r_1 = 1.78$ and $r_2 = 0.67$ values were obtained. In a similar manner, $r_1 = 0.88$ and $r_2 = 0.36$ values were observed for the copolymerization of (*R*)-MOHEL with PL. Thus, the monomer reactivity ratio of (*R*)-MOHEL exceeds that of VL and PL while the monomer reactivity ratio of (*R*)-MOHEL is lower than that of CL. Therefore, the resulting poly[(*R*)-MOHEL-*ran*-VL] and poly[(*R*)-MOHEL-*ran*-PL] exhibit highly block like arrangements when the polymerizations are conducted to high conversions. In fact, poly[(*R*)-MOHEL-*ran*-PL] (60/40) exhibits a relatively small MOHEL/MOHEL/PL or MOHEL/PL/MOHEL (MMP* or MP*M) sequence and small PPM* or PM*P sequence compared with MMM and PPP sequences as evidenced by ¹³C NMR spectroscopy (Figure 1). In a similar manner, poly[(*R*)-MOHEL-*ran*-VL] (62/38) shows a relatively small VL/VL/MOHEL or VL/MOHEL/VL sequence (VVM* or VM*V) and MV*M or MMV* sequence compared with VVV and MMM se-

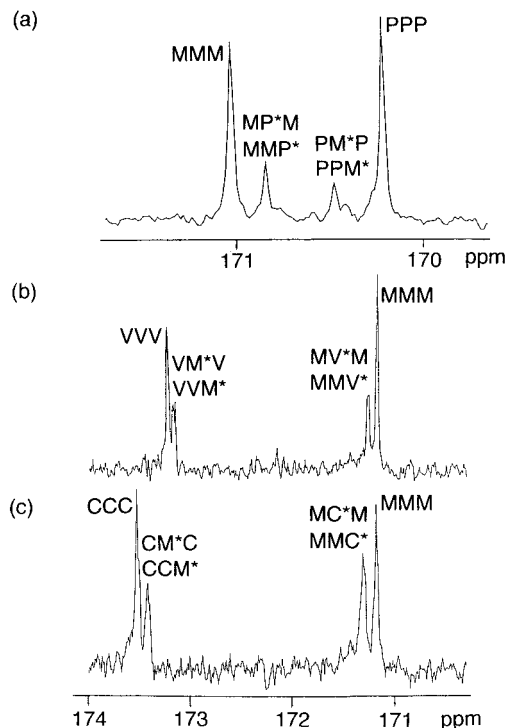


Figure 1. ¹³C NMR spectra of carbonyl region of (a) poly[(*R*)-MOHEL-*ran*-PL], (b) poly[(*R*)-MOHEL-*ran*-VL], and (c) poly[(*R*)-MOHEL-*ran*-CL].

quences. However, poly[(*R*)-MOHEL-*ran*-CL] (48/52) shows the relatively large MOHEL/MOHEL/CL or MOHEL/CL/MOHEL sequence (MMC* or MC*M) and large CCM* or CM*C sequence compared with CCC and MMM sequences. Homo-poly[(*R*)-MOHEL], poly(PL), poly(VL), and poly(CL) exhibit carbonyl carbon resonances at 171.18, 170.22, 173.32, and 173.51 ppm, respectively, in their ¹³C NMR spectra.

Biodegradation by Activated Sludge. In natural environments, biodegradation of polymeric materials generally occurs by activated sludge in municipal sewage plants, bacteriophages in rivers, activities of microorganisms in sea water, and/or activities of protists in soil. Therefore biodegradation of solid masses of the new polymers with acclimated activated sludge containing mainly nitrification bacteria was first examined. Solid masses of polymers (thickness 1 mm × 5 mm × 5 mm) were used here to examine the relative biodegradability of poly[(*R*)-MOHEL] and poly[(*R*)-MOHEL-*ran*-CL] (91/9), which exhibit no film formation ability due to their low T_g . When the lactone component becomes rich (>ca. 60%) in the copolymers, we could use the sample as films. As a consequence, biodegradability of random (*R*)-MOHEL/CL copolymers increases with an increase of the CL component and shows the maximum value when the constitution becomes 24/76 resulting in 60% loss of the original polymer in 30-40 days (Figure 2). Biodegradability increases in the order 24/76 > 48/52 > 73/27 > 9/91 = 91/9 of the (*R*)-MOHEL/CL random copolymers.

The biodegradability of poly[(*R*)-MOHEL-*ran*-VL] and poly[(*R*)-MOHEL-*ran*-PL] (4/90-60/40) is much smaller (only <5% weight loss after 30 days) compared with that of poly[(*R*)-MOHEL-*ran*-CL]. The biodegradability of these polymers was also lower than that of homopoly[(*R*)-MOHEL] (ca. 50% weight loss after 40 days). This result may come from preferred block arrangement of (*R*)-MOHEL and PL or VL polymers in the copolymers. Furthermore, the biodegradability of poly(3-HB-*ran*-3-

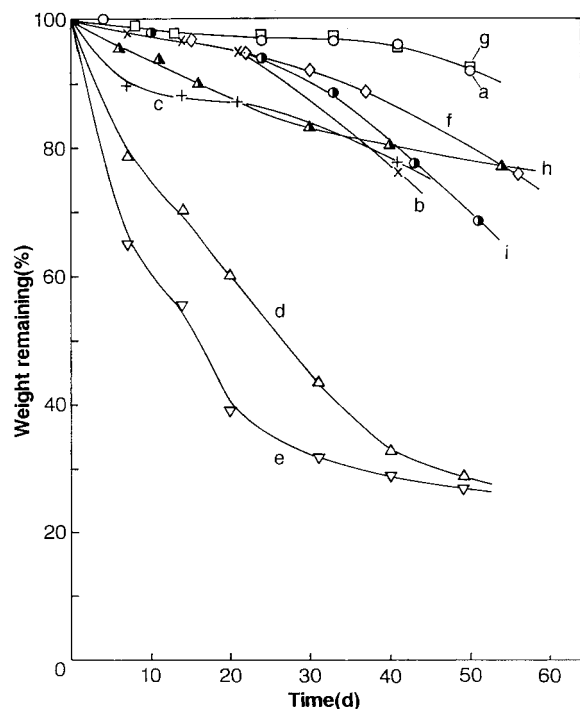


Figure 2. Biodegradation of polyesters (solid masses) by acclimated activated sludge: (a) poly[(*R*)-MOHEL], (b) poly[(*R*)-MOHEL-*ran*-CL] (91/9), (c) 73/27 ratio, (d) 48/52 ratio, (e) 24/76 ratio, (f) 9/91 ratio, (g) poly(CL), (h) poly[(*R*)-MOHEL-*block*-poly(CL)] (49/51), (i) poly(3-HB-*ran*-3-HV) (89/11).

HV) (89/11) was much lower compared with that of poly[(*R*)-MOHEL-*ran*-CL] as shown in Figure 2. In contrast to the behavior of random (*R*)-MOHEL/lactone copolymers, biodegradability of the block copolymer of (*R*)-MOHEL/CL (49/51) is significantly lower with acclimated activated sludge. This result may be straightforwardly correlated to the low degradability of homopolymers, both poly[(*R*)-MOHEL] and poly(CL).

To understand the dependence of biodegradability by acclimated activated sludge on the stereostructures of polymers, the biodegradations of (*R*), (*S*), and racemic poly(MOHEL) were compared. The biodegradability of poly[(*R*)-MOHEL] is higher (17% loss after 80 days) than that of poly(*rac*-MOHEL) (9% loss after 80 days) and poly[(*S*)-MOHEL] (only 2% after 80 days). These results indicate that poly[(*R*)-MOHEL] exhibits the highest biodegradability. However, it should be noted that even racemic polymer shows fairly good biodegradability. This finding indicates that even nonchiral copolymers such as poly(4-oxa-6-hexanolide-*ran*-CL) or poly(4-oxa-6-hexanolide-*ran*-VL) should show rather good biodegradability.

Biodegradability of poly[(*R*)-MOHEL-*ran*-CL] by normal activated sludge under aerobic or anaerobic conditions gave different results. Especially noteworthy is that biodegradation under aerobic conditions occurred preferentially after 20 days, but the remaining weight of polymers under anaerobic conditions is higher than that by biodegradation under aerobic conditions (Figure 3). Thus biodegradation under aerobic conditions is preferable for these types of polyesters. The reason why acclimated sewage effects sample degradation differently than normal sludge may come from higher values of DO (dissolved oxygen; 5 ppm), higher values of MLSS (mixed liquor suspended solid; 3500 mg/L), and the presence of different kinds of microorganisms (mainly nitrification bacteria) for the acclimated sewage.

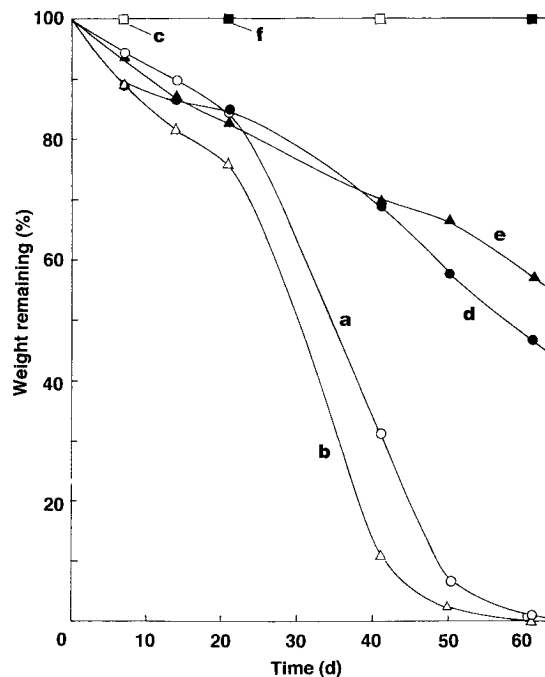


Figure 3. Biodegradation of polyester films by normal activated sludge. Aerobic conditions: (a) poly[(*R*)-MOHEL-*ran*-CL] (0/100), (b) 24/76 ratio, (c) 48/52 ratio. Anaerobic conditions: (d) poly[(*R*)-MOHEL-*ran*-CL] (0/100), (e) 24/76 ratio, (f) 48/52 ratio.

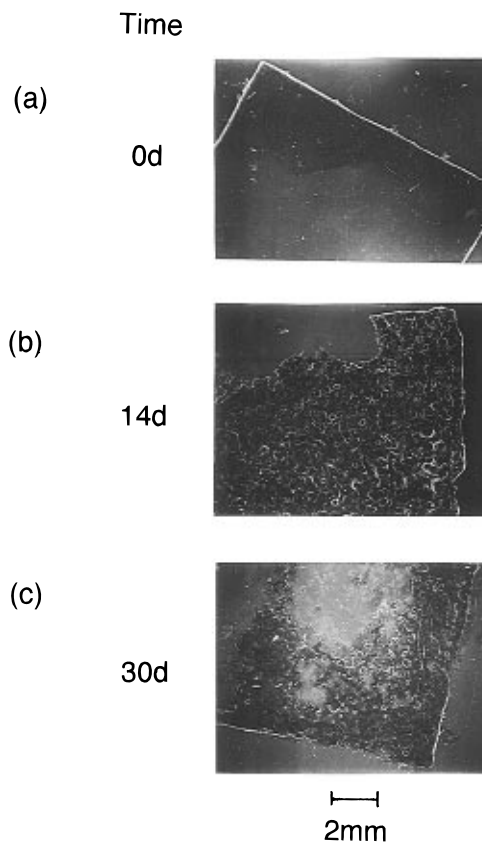


Figure 4. SEM images of poly[(*R*)-MOHEL-*ran*-CL] (48/52) film before and after biodegradation by normal activated sludge: (a) before degradation, (b) after 14 days, (c) after 30 days.

SEM images of poly[(*R*)-MOHEL-*ran*-CL] (48/52 molar ratio) films before and after biodegradation by acclimated active sludge are given in Figure 4. During the immersion of the sample in acclimated sludge for

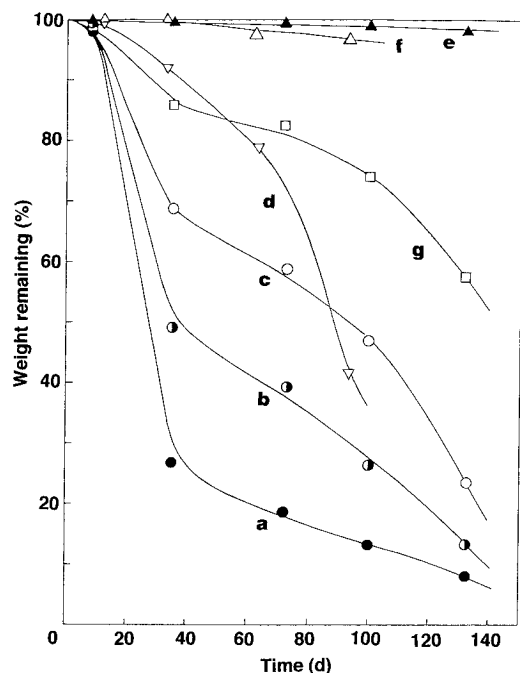


Figure 5. Biodegradation of poly[(*R*)-MOHEL-*ran*-CL] and poly[(*R*)-MOHEL-*ran*-VL] films by sea water: (a) poly[(*R*)-MOHEL-*ran*-CL] (14/86), (b) 9/91 ratio, (c) 4/96 ratio, (d) poly(CL), (e) poly[(*R*)-MOHEL-*ran*-VL] (22/78), (f) poly(VL), (g) poly(3-HB-*ran*-3-HV) (89/11).

14 days, many small cavities (diameter 200 nm) opened on the surface of films. The cavities further developed during the next 30 days (remaining weight is 13–15%). However, significant weight loss was not observed in case of poly[(*R*)-MOHEL-*ran*-PL] (31/69), i.e., only 20 wt% loss was observed after 50 days.

The biodegradations of poly[(*R*)-MOHEL-*ran*-CL] copolymers in sea water at 11–25 °C showed significant weight loss especially when the copolymer was composed of a 14/86 or 9/91 ratio (Figure 5). The sea water should contain some microorganisms. The experiment was carried out at the 2 m depth of Inland Sea. The sample was weighed at a fixed time interval and was held in a polyethylene network to expose it to the sea water. In contrast to the behavior of (*R*)-MOHEL/CL random copolymer, the (*R*)-MOHEL/VL (62/38) and (*R*)-MOHEL/PL (60/40) random copolymers are almost inert to sea water (only 2–3 wt % loss of (*R*)-MOHEL/VL or (*R*)-MOHEL/PL random copolymers was observed after 140 days). Biopol [poly(3-HB-*ran*-3-HV) (89/11)] also showed relatively small biodegradability in sea water. The number-averaged molecular weights and the molecular weight distributions of (*R*)-MOHEL/CL random copolymers did not change after biodegradation by sea water (Table 2). This means that biodegradation starts from the polymer surface and the random scission of polymer chains occurred. Thus the inside of the polymer materials remained unchanged, while the biodegradation occurred at the surface of the polymer. However, in the case of poly[(*R*)-MOHEL], poly(CL), and poly(PL), the number-averaged molecular weight decreased after the biodegradation. Thus, the biodegradation of these polymers occurred inside of the polymer material (amorphous part) to broaden the M_w/M_n .

Photographs of various poly[(*R*)-MOHEL-*ran*-CL] before and after degradation by sea water are shown in Figure 6. The biodegradability increases with an increase of MOHEL content in the resulting polymers. Therefore, poly[(*R*)-MOHEL-*ran*-CL] (14/86) almost dis-

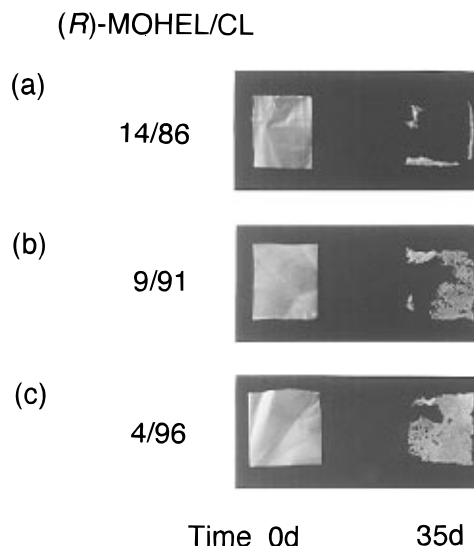


Figure 6. Photographs of poly[(*R*)-MOHEL-*ran*-CL] films before and after degradation by sea water.

Table 2. Change in Molecular Weight (Distribution) of Polyesters before and after Biodegradation in Sea Water

copolymer	time (day)	wt remaining/%	$M_{no}/\times 10^3$	$M_{nt}/\times 10^3$	M_w/M_n	M_w/M_n
poly[(<i>R</i>)-MOHEL/CL]						
14/86	35	26.6	248	221	1.96	1.84
9/91	35	49.1	287	230	1.91	1.55
4/96	35	68.8	279	249	1.90	1.75
poly[(<i>R</i>)-MOHEL/PL]						
60/40	9	48.4	107	60	2.25	2.25
poly[(<i>R</i>)-MOHEL]	9	85.2	118	48	1.82	3.78
poly(CL)	9	87.3	138	52	1.26	3.40
poly(PL)	9	92.1	92	22	2.30	3.35

appeared after 35 days exposure, while biodegradation of poly[(*R*)-MOHEL-*ran*-CL] (4/96) resulted in the remaining of significant quantities of solid masses.

Hydrolytic degradations of polyesters were measured in phosphatase buffer at pH 7.1 and 1.1 at 37 °C, i.e., (*R*)-MOHEL/CL random copolymers (73/27, 48/52, 24/76) are resistant to hydrolytic degradation, while the decomposition at pH 12.8 at 37 °C resulted in a significant weight loss of the block copolymer [(*R*)-MOHEL/CL = 49/51] and homopolymer of (*R*)-MOHEL (Figure 7). Only 10 wt % of these polymers remained after 20 days decomposition under these conditions. The homopolymer of CL also degrades hydrolytically to result in ca. 80% degradation in 30 days at pH 12.8. The homopolymer of PL and random copolymer of (*R*)-MOHEL/PL (60/40) are inert to hydrolytic degradation at pH 5.6, 7.2, and 9.0 (not shown in the figures).

Biodegradation of (*R*)-MOHEL/Lactone Copolymers by Enzymes. Biodegradation of solid masses of (*R*)-MOHEL/CL random copolymers by cholesterol esterase (from *Pseudomonas* sp.) is shown in Figure 8. We have used the solid masses again here because poly[(*R*)-MOHEL-*ran*-CL] (88/12) and homopolymer poly[(*R*)-MOHEL] are too soft to form the films at ambient temperatures. Biodegradation increases with increase of ϵ -caprolactone content in the resulting copolymers (52–76%), although poly[(*R*)-MOHEL] and poly(CL) homopolymers themselves are inert to cholesterol esterase. In contrast, biodegradation of poly[(*R*)-MOHEL-*block*-CL] (49/51 ratio) occurs only slightly and the behavior of biodegradation resembles that of homopolymers poly[(*R*)-MOHEL] and poly(CL). As a whole, the amount of biodegradation resembles that by acclimated activated sludge.

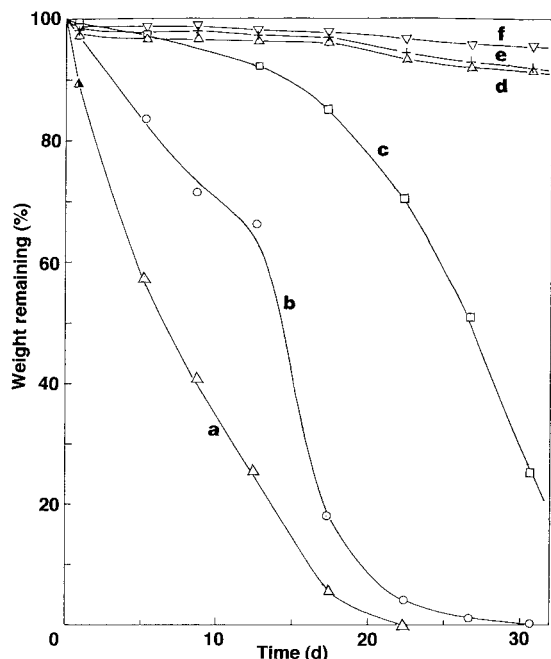


Figure 7. Hydrolytic degradation of polyester films in alkaline aqueous solution (pH 12.8, 37 °C): (a) poly[(*R*)-MOHEL-*block*-poly(CL)] (49/51), (b) poly[(*R*)-MOHEL], (c) poly(CL), (d) poly[(*R*)-MOHEL-*ran*-CL] (48/52), (e) 73/27 ratio, f) 24/76 ratio.

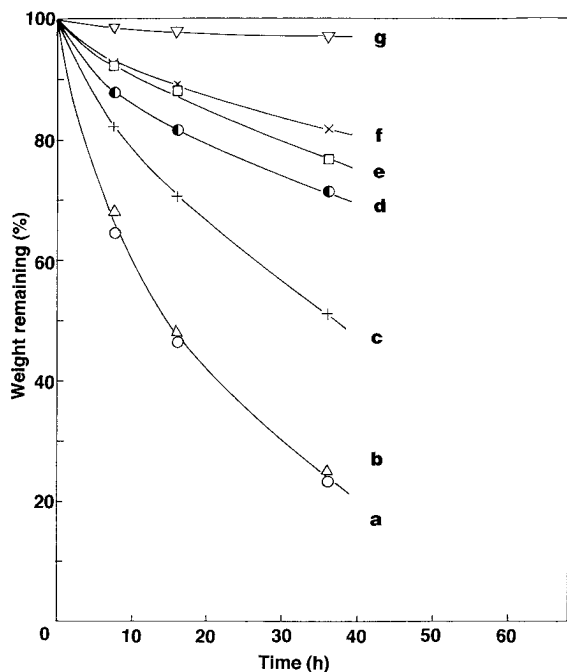


Figure 8. Biodegradation of solid masses of poly[(*R*)-MOHEL-*ran*-CL] and poly[(*R*)-MOHEL]-*block*-poly(CL) by cholesterol esterase (from *Pseudomonas* sp.): (a) poly[(*R*)-MOHEL-*ran*-CL] (48/52), (b) 24/76 ratio, (c) 73/27 ratio, (d) poly[(*R*)-MOHEL]-*block*-poly(CL) (49/51), (e) poly(CL), (f) poly[(*R*)-MOHEL-*ran*-CL] (88/12), (g) poly[(*R*)-MOHEL].

Biodegradation of random copoly[(*R*)-MOHEL/CL] with three kinds of lipases was also explored. The activity increases in the order *Chromobacterium viscosum* > *Rhizopus delemar* ≥ *Candida cylindracea*. In case of *C. cylindracea*, only 5 wt % decomposition was observed after 50 h. The biodegradation of poly[(*R*)-MOHEL-*ran*-CL] and poly[(*R*)-MOHEL]-*block*-poly(CL) by *C. viscosum* is given in Figure 9. The weight loss of polymers increases with increase of CL unit in the copolymers in the order 24/76 > 48/52 > 73/27 > 88/12

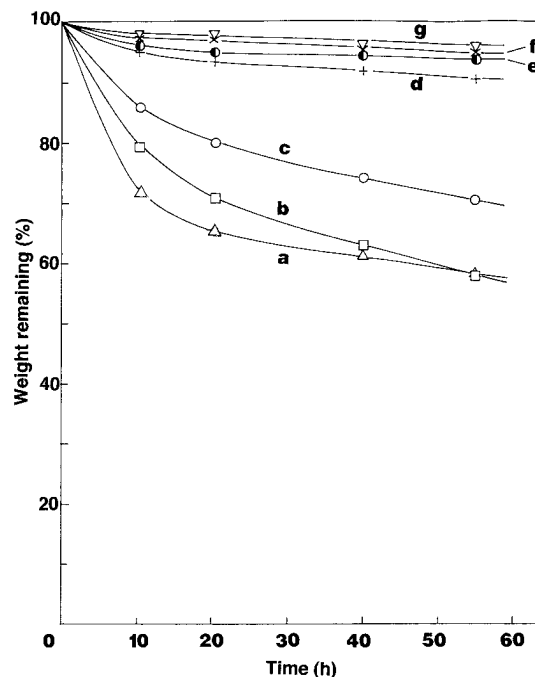


Figure 9. Biodegradation of solid masses of poly[(*R*)-MOHEL-*ran*-CL] and poly[(*R*)-MOHEL]-*block*-poly(CL) by *C. viscosum* lipase: (a) poly[(*R*)-MOHEL-*ran*-CL] (24/76), (b) poly(CL), (c) poly[(*R*)-MOHEL-*ran*-CL] (48/52), (d) poly[(*R*)-MOHEL-*ran*-CL] (73/27), (e) poly[(*R*)-MOHEL]-*block*-poly(CL) (49/51), (f) poly[(*R*)-MOHEL-*ran*-CL] (88/12), (g) poly[(*R*)-MOHEL].

ratio of (*R*)-MOHEL/CL. However, poly(CL) also decomposes significantly. Especially, poly(CL) with $M_n = 26\,000$ decomposes >90 wt % in 24 h by using a 4 times higher concentration of *C. viscosum*. Thus, poly(CL) shows high biodegradation with *C. viscosum* since this type of lipase exhibits good affinity toward poly(CL).

The pH change of the solution ($-\Delta\text{pH}/(\text{g of polyester})$) obtained from biodegradation of poly[(*R*)-MOHEL-*ran*-CL] (14/86) film and poly[(*R*)-MOHEL-*ran*-VL] (22/78) film by cholesterol esterase was also observed (Figure 10). The (*R*)-MOHEL/CL (14/86) random copolymer decomposes in 80–90 wt % to result in strong acidity of the degradation solution, while CL and VL homopolymers take a little decomposition under the same reaction conditions. The pH change of the solution obtained from biodegradation of poly[(*R*)-MOHEL-*ran*-CL] (14/86) film and poly[(*R*)-MOHEL-*ran*-VL] (22/78) film was also tested with *C. viscosum* lipase (Figure 11). The films are gradually decomposed upon treatment by lipase in buffer solution. About 90 wt % of the (*R*)-MOHEL/CL (14/86) copolymer film decomposes in 20 h, and 90 wt % of (*R*)-MOHEL/VL film decomposes in 70 h.

Biodegradation of 60/40 poly[(*R*)-MOHEL-*ran*-PL] with cholesterol esterase, lipase B (*Pseudomonas fragi* 22-39B), and *R. delemar* lipase was carried out in $\text{Na}_2\text{HPO}_4\text{--KH}_2\text{PO}_4$ or $\text{CH}_3\text{COONa--HCl}$ buffer solution at pH 5.6–9.9 (Figure 12). As a result, cholesterol esterase shows the highest degradation ability (60% of polymer degraded in 400 h), while the lipase enzymes show a little degradation. To understand the effect of molar ratio between (*R*)-MOHEL and PL on the biodegradation of the copolymers, degradation of solid masses of 100/0, 81/19, 60/40, and 31/69 poly[(*R*)-MOHEL-*ran*-PL] and PL homopolymer were examined with cholesterol esterase. Both high molecular weight ($9.2 \times 10^4 < M_n < 12.3 \times 10^4$) and low molecular weight ($8.6 \times 10^3 < M_n < 13.9 \times 10^3$) copolymers were used as the samples.

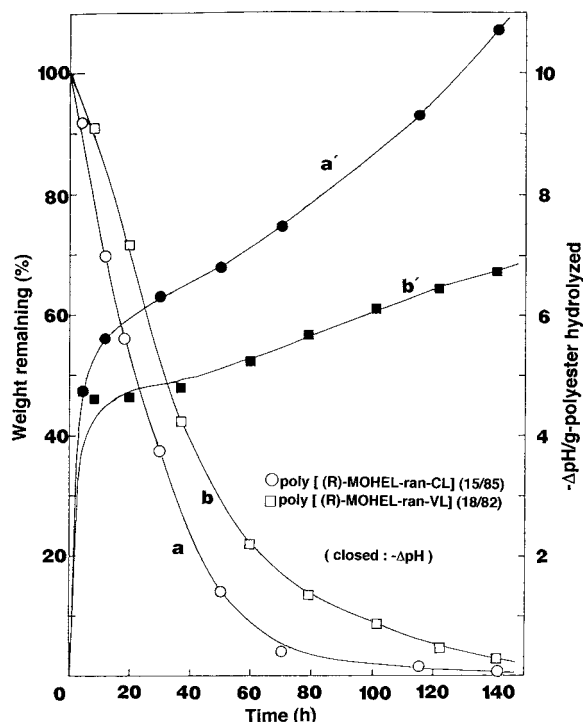


Figure 10. pH change of the solution obtained by enzymatic degradation of (a) poly[(*R*)-MOHEL-*ran*-CL] (14/86) film and (b) poly[(*R*)-MOHEL-*ran*-VL] (22/78) film with cholesterol esterase.

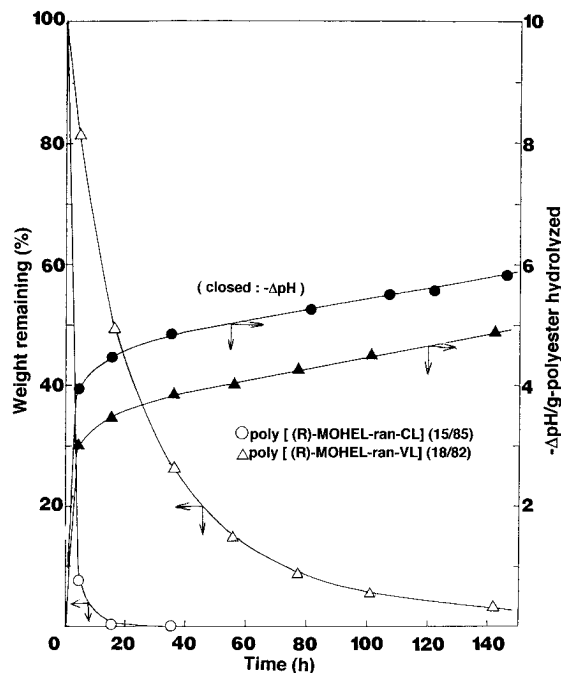


Figure 11. pH change of the solution obtained by biodegradation of (a) poly[(*R*)-MOHEL-*ran*-CL] (14/86) film and (b) poly[(*R*)-MOHEL-*ran*-VL] (22/78) film with *C. viscosum*.

As a result, biodegradation of 60/40 and 81/19 copolymers of high molecular weight polymers ($90\,000 < M_n < 120\,000$) occurred preferentially, and the weight remaining was 40% in the case of the 60/40 copolymer, while the 31/69 copolymer showed little decomposition (Figure 13). The biodegradation of 60/40 copolymer with lipasae B (*P. fragi* 22-39E) and *R. delemar* lipase resulted in less decomposition. In the case of low molecular weight copolymers, 74/26 copolymer degraded better than the copolymer of 58/42 molar ratio. Thus,

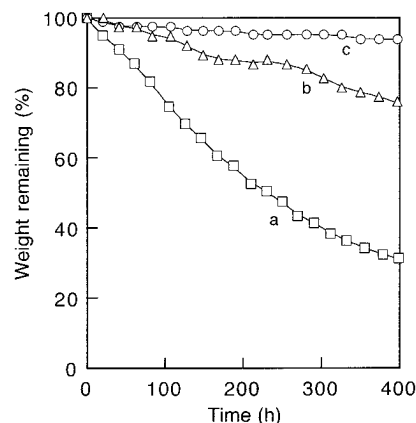


Figure 12. Biodegradation of poly[(*R*)-MOHEL-*ran*-PL] (60/40) film by (a) cholesterol esterase, (b) *P. fragi*, and (c) *R. delemar*.

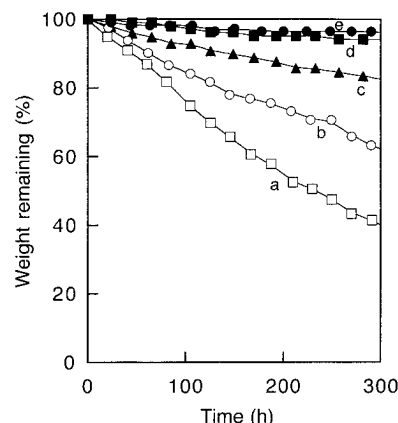


Figure 13. Biodegradation of solid masses of poly[(*R*)-MOHEL-*ran*-PL] by cholesterol esterase. (a) poly[(*R*)-MOHEL-*ran*-PL] (60/40), (b) 81/19 ratio, (c) poly[(*R*)-MOHEL], (d) poly[(*R*)-MOHEL-*ran*-PL] (31/69), (e) poly(PL).

low molecular weight polymers degraded faster than high molecular weight polymers. The physical change of poly[(*R*)-MOHEL-*ran*-PL] (60/40) after enzymatic degradation with cholesterol esterase lies in a decrease of molecular weight from $M_n = 10.7 \times 10^4$ to 6.01×10^4 while M_w/M_n remains intact. This means that relatively low molecular weight polymer portions of the copolymers decompose preferentially. The role of temperature for the biodegradation by enzymes was not checked because we employed here the most suitable conditions (37–65 °C) which show the maximum biodegradation.

Photographs of poly[(*R*)-MOHEL-*ran*-PL] (60/40) after biodegradation by cholesterol esterase are shown in Figure 14. The weight loss is 36% based on the original polymer, and many cavities are observed in the form of slits. Accelerated opening of such slits developed further by holding the sample in the enzymatic solution.

After carefully comparing the degradability of blended polymer [(*R*)-MOHEL/PL] (50/50) with that of (*R*)-MOHEL homopolymer using cholesterol esterase, lipase B, and *R. delemar* lipase, no significant degradation was observed in either.

Analysis of Degraded Products. Figure 15 shows the HPLC profiles of water-soluble products of (*R*)-MOHEL/CL (15/85) and (*R*)-MOHEL/VL (18/82) random copolymers degraded by cholesterol esterase. Obviously, (*R*)-MOHEL/CL copolymer degraded into a lower molecular weight product compared with that of (*R*)-MOHEL/VL copolymer. Finally we separated these products by HPLC and analyzed each fraction by NMR

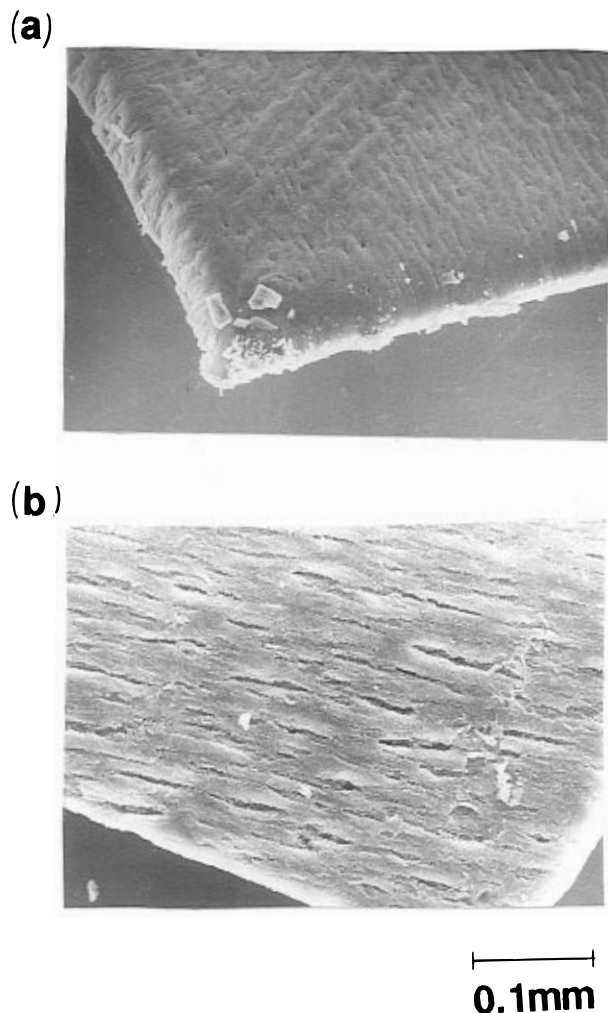


Figure 14. Photographs of poly[(*R*)-MOHEL-*ran*-PL] (a) before and (b) after enzymatic degradation by cholesterol esterase (106 h).

spectroscopy and mass spectrometry. The ^1H NMR spectrum for the lowest molecular weight fraction of water-soluble products derived from poly[(*R*)-MOHEL-*ran*-CL] is that of 6-hydroxycaproic acid. The second lowest molecular weight fraction is composed of two products (Figure 16). One is the caproic acid dimer, and the other is 1/1 addition compound of caprolactone with (*R*)-MOHEL in a 14/3 ratio. In a similar manner, the second lowest molecular weight product derived from poly[(*R*)-MOHEL-*ran*-VL] (18/82) was isolated and was found to be valeric acid dimer as revealed by its ^1H NMR spectrum. The lowest molecular weight product should be 5-hydroxyvaleric acid, but we have failed to isolate this product because of its low yield. Biodegradation of poly[(*R*)-MOHEL] by cholesterol esterase gives water-soluble oligomers composed of at least three components, which we are unable to identify.

Experimental Section

General. ^1H and ^{13}C NMR spectra were recorded on a JEOL EX-270 spectrometer or a Bruker AM-X400wb spectrometer. Chemical shifts were calibrated using chloroform in chloroform- d_3 at 7.26 ppm for ^1H NMR spectra and 77.0 ppm for ^{13}C NMR spectra. Number-averaged molecular weights and molecular weight distributions of polymers were determined by gel permeation chromatography on a Tosoh SC-8010 high-speed liquid chromatograph equipped with a differential refractometer detector, using CHCl_3 as eluent at 40 $^\circ\text{C}$. The columns were TSK gel G5000H, G4000H, G3000H,

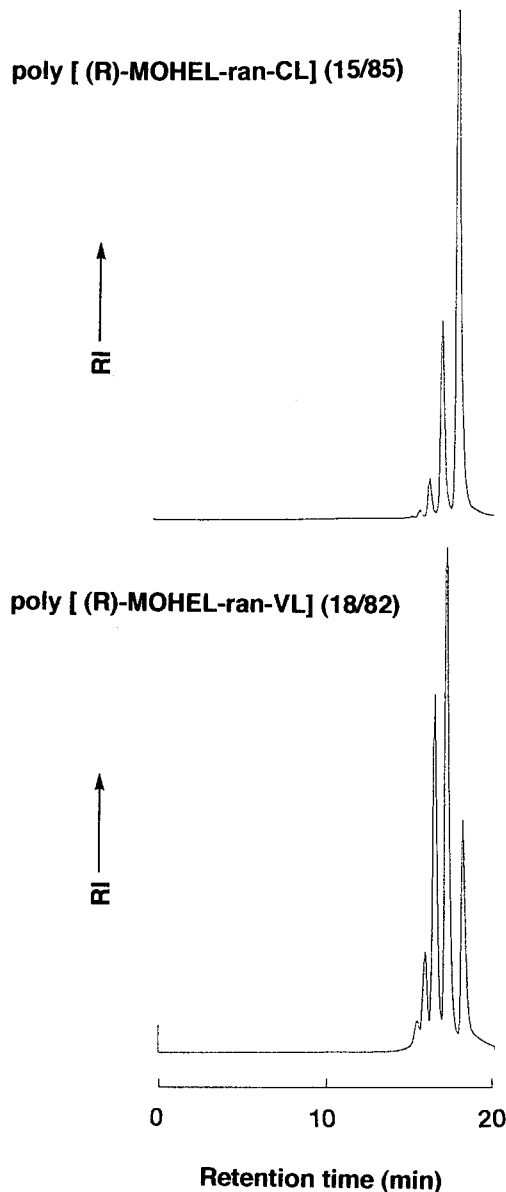


Figure 15. High-performance liquid chromatographic profiles of degraded products obtained from (a) poly[(*R*)-MOHEL-*ran*-CL] (15/85) film and (b) poly[(*R*)-MOHEL-*ran*-VL] (18/82) film.

and G2000H. The flow rate was 1.0 mL min^{-1} . The molecular weights were determined by using a universal curve plotted with standard polystyrene, whose M_w values were measured by a light-scattering method. T_g and T_m were measured on a Shimadzu DSC-50, and mechanical properties of polymers were determined by a Shimadzu autograph AGS-500B.

Materials. (*R*)- and (*S*)-3-methyl-4-oxa-6-hexanolide (MOHEL) (ee = 97%, $[\alpha]_D = -14.2^\circ$ ($c = 1.0$, CHCl_3 , 20 $^\circ\text{C}$) and $+14.1^\circ$) prepared from the reaction of (*R*)- or (*S*)-3-(2-hydroxyethoxy)hydroxybutyric acid with ethyl chloroformate were provided by Takasago Research Institute and were dried over CaH_2 and then over CaCl_2 . Lactones such as ϵ -caprolactone, δ -valerolactone, and β -propiolactone were purchased from Aldrich Chemical Co. and were dried over CaH_2 , then anhydrous CaCl_2 and distilled before use.

Polymerization of Lactones. Homopolymerizations of (*R*)- or (*S*)-MOHEL, ϵ -caprolactone, δ -valerolactone, and β -propiolactone and copolymerizations of these monomers were conducted using $\text{AlEt}_3\text{-H}_2\text{O}$ (1/0.8) as an initiator (1.0 mol % of monomer) in toluene. The mixture was heated to 60 $^\circ\text{C}$ for 10 days. The resultant polymers were poured into MeOH to induce the precipitation of polymers. The polymers thus obtained were dissolved in CHCl_3 , and the solutions were again poured into MeOH. The random (*R*)-MOHEL/CL copolymers

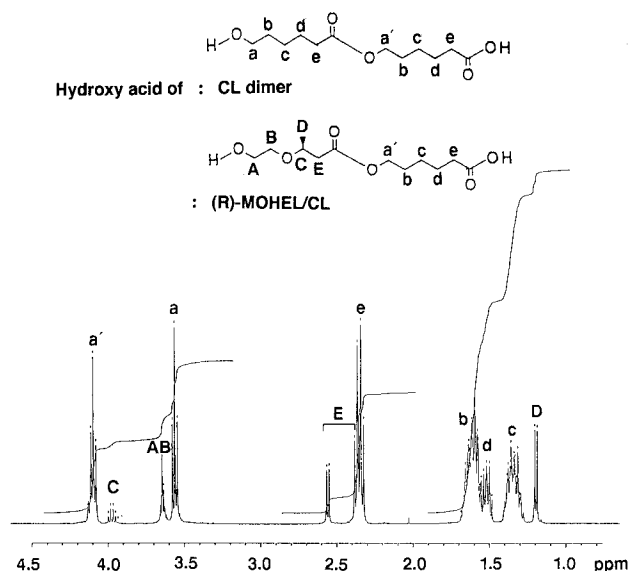


Figure 16. ^1H NMR spectrum of caproic acid dimer and (*R*)-MOHEL/CL obtained from biodegradation of poly[(*R*)-MOHEL-*ran*-CL] (15/85).

of 24/76, 48/52, and 72/28 ratios showed $[\alpha]_D$ (CHCl_3 , 25 °C) of -9.2° , -14.0° , and -22.4° , and the random (*R*)-MOHEL/VL copolymers of 35/65, 62/38, and 84/16 ratios showed $[\alpha]_D$ of -11.4° , -19.2° , and -23.6° , respectively. In a similar manner, the random copolymers of (*R*)-MOHEL/PL in 34/66, 60/40, and 83/27 ratios showed $[\alpha]_D$ -12.1° , -20.0° , and -24.1° , respectively. The homopolymer of (*R*)-MOHEL showed $[\alpha]_D$ of 26.8° .

Biodegradations by Activated Sludge. Biodegradations of homopolymers and copolymers were conducted using normal activated sludge at 20 °C at the Higashi-Hiroshima water purification center. The pH was adjusted to ca. 6. The DO value was ca. 3 ppm under aerobic conditions and 0.2–0.3 ppm under anaerobic conditions. The MLSS was 2800 mg/L in both cases. Degradation of films (10–50 mg) by acclimated activated sludge was also explored at 20 °C at pH 8–9. The DO value was ca. 5 ppm and MLSS 3500 mg/L.

Biodegradations by Enzymes. Biodegradations by enzymes were carried out by using the enzyme concentration of 1.0 unit/(mg of polyester). The cholesterol esterase from *Pseudomonas* sp., lipase from *R. delemar*, and lipase from *C. viscosum* were purchased from Wako Pure Chemical Industry. The conditions employed here for the enzymatic degradations were as follows: *R. delemar* lipase (pH 5.6, acetic acid buffer, 40 °C); *C. viscosum* lipase (pH 6.8, 65 °C); and *Pseudomonas* sp. cholesterol esterase (pH 7.0, 37 °C). Polymer films (thickness 50–70 μm , 5 mm \times 5 mm) were allowed to settle in the enzymatic solution and were stirred magnetically during all experiments.

Biodegradations by Sea Water. Decomposition of the samples in sea water was carried out by sinking the films (50–200 mg) to a depth of 1.5 m of Inland Sea (pH 8.2) at Otake at 10–25 °C, using a polyethylene network (1 \times 1 mm mesh) in a stainless cage. In every case, six samples were used for one examination and averaged weight loss was determined.

Analysis of Biodegradation Product. Water-soluble fractions of biodegradation product by enzymes were filtered and lyophilized. The solid masses were then washed with a

mixture of THF/diethyl ether to remove the enzyme and buffer. The resulting organic solvent soluble fraction was separated using preparative HPLC (Nihon Bunko System 800, column TSKgel G2000H, column temperature 40 °C, detector differential refractometer) and analyzed by ^1H NMR spectroscopy and mass spectrometry.

References and Notes

- (1) (a) Pool, R. *Science* **1989**, *245*, 1187. (b) Ramsey, J. A.; Ramsey, B. A. *Appl. Physiol. Forum* **1990**, *7*, 1. (c) King, P. P. *J. Chem. Technol. Biotechnol.* **1982**, *32*, 2. (d) McCarthy-Bates, L. *Plastic World* 1993, March 22.
- (2) Chasin, M.; Langer, L., Eds. Biodegradable Polymers as Drug Delivery Systems. *Drugs Pharm. Sci.* **1990**, *45*, 162, 231.
- (3) (a) Chasin, M.; Langer, L., Eds. Biodegradable Polymers as Drug Delivery Systems. *Drugs Pharm. Sci.* **1990**, *45*, 141. (b) Lipinsky, E. S.; Sinclair, R. G. *Chem. Eng. Prog.* **1986**, *82*, 26.
- (4) (a) Cohn, D.; Younes, H. *J. Biomed. Mater. Res.* **1988**, *22*, 993. (b) Schakenraad, J. M.; Nieuwenhuis, P.; Molenaar, I.; Helder, J.; Dijkstra, P. J.; Feijen, J. *J. Biomed. Mater. Res.* **1989**, *23*, 1271. (c) Gassner, F.; Owen, A. J. *Polymer* **1994**, *35*, 2233. (d) Muller, D.; David, A.; Muhr, G. *J. Mater. Sci.: Mater. Med.* **1995**, *6*, 68. (e) Cerrai, P.; Tricoli, M. *Makromol. Chem., Rapid Commun.* **1993**, *14*, 529. (f) Cerrai, P.; Tricoli, M.; Lelli, L.; Guerra, G. D.; Guerra, R. S.; Cascone, M. G.; Giusti, P. *J. Mater. Sci.: Mater. Med.* **1994**, *5*, 308. (g) Suuronen, S.; Pohjonen, T.; Taurio, R.; Tormala, P.; Wessman, L.; Ronkko, K.; Vainnnionpaa, S. *J. Mater. Sci.: Mater. Med.* **1992**, *3*, 426. (h) Davis, P. A.; Huang, S. J.; Ambrosio, L.; Ronca, D.; Nicolais, L. *J. Mater. Sci.: Mater. Med.* **1991**, *3*, 359.
- (5) (a) Nomura, R.; Ueno, A.; Endo, T. *Macromolecules* **1994**, *27*, 620. (b) Inoue, S.; Tomoi, Y.; Tsuruta, T.; Furukawa, J. *Makromol. Chem.* **1961**, *48*, 229. (c) Jedlinski, Z.; Kowalczyk, M.; Kurock, P. *Makromol. Chem., Macromol. Symp.* **1986**, *3*, 277.
- (6) (a) Teranishi, K.; Iida, M.; Araki, T.; Yamashita, S.; Tani, H. *Macromolecules* **1974**, *7*, 421. (b) Teranishi, K.; Araki, T.; Tani, H. *Macromolecules* **1972**, *5*, 660.
- (7) (a) Yasuda, T.; Aida, T.; Inoue, S. *Bull. Chem. Soc. Jpn.* **1986**, *59*, 3931. (b) Shimasaki, K.; Aida, T.; Inoue, S. *Macromolecules* **1987**, *20*, 3076. (c) Endo, M.; Aida, T.; Inoue, S. *Macromolecules* **1987**, *20*, 2982.
- (8) Vergara, J.; Figini, R. V. *Makromol. Chem.* **1977**, *178*, 267.
- (9) (a) Okuda, J.; Rushkin, I. L. *Macromolecules* **1993**, *26*, 5530. (b) Okuda, J.; Kleinhenn, T.; Konig, P.; Taden, I.; Ngo, S.; Rushkin, I. L. *Macromol. Symp.* **1995**, *95*, 195.
- (10) (a) McLain, S. J.; Drysdale, N. E. U.S. Patent 5,028,667, 1991 (assigned to E. I. du Pont de Nemours and Co.). (b) McLain, S. J.; Ford, T. M.; Drysdale, N. E. *Polym. Prepr.* **1992**, *33*, 463. (c) McLain, S. J.; Drysdale, N. E. *Abstracts of Papers*, 203rd National Meeting of the American Chemical Society, San Francisco, CA, April 1992; American Chemical Society: Washington, DC, 1992; POLY-160. (d) Yamashita, M.; Take moto, Y.; Ihara, E.; Yasuda, H. *Macromolecules* **1996**, *29*, 1798.
- (11) (a) Evans, W. J.; Katsumata, H. *Macromolecules* **1994**, *27*, 2330. (b) Evans, W. J.; Katsumata, H. *Macromolecules* **1994**, *27*, 4011.
- (12) (a) Uyama, H.; Takeya, K.; Kobayashi, S. *Bull. Chem. Soc. Jpn.* **1995**, *68*, 56. (b) MacDonald, R. T.; Pulapura, S. K.; Svirkin, Y. Y.; Gross, R. A.; Kaplan, D. L.; Akkara, J.; Swift, G.; Wolk, S. *Macromolecules* **1995**, *28*, 73.
- (13) (a) Hori, Y.; Suzuki, M.; Yamaguchi, A.; Nishisita, T. *Macromolecules* **1993**, *26*, 5533. (b) Hori, Y.; Yamaguchi, A. *Macromolecules* **1995**, *28*, 406.

MA951759B